Comparison of Large Phased Arrays Using Stacked Segments

W. Driesel[1], A. Pampel[1], T. Mildner[1], S. Hetzer[1], and H. E. Möller[1]

[1]Max Planck Institute for Human Cognitive and Brain Sciences, Leipzig, Germany

Introduction

It is well known that multi-channel phased arrays are well-suited for parallel imaging. An optimum signal-to-noise ratio (SNR) performance is achieved if the geometry of the coils employed assures a maximum $\mathbf{B}_1$-field sensitivity in the field-of-view (FOV) and minimizes the electric coupling coefficient between different coils in the array. The fundamental goal in the development of large phased arrays is thus to meet these two demands. The stacked segment (1) with a loop, and a microstrip transmission-line (MTL) antenna may be a good choice as a basic segment for an array because its elements are all geometrically decoupled (~30dB). However, electric coupling between different segments arranged e.g. on a cylinder may lead to a suboptimal SNR. Therefore, simulations of several stack configurations were performed to further optimize the design.

Methods

Two array configurations were compared: (A) an array with 16 loops and 16 MTLs; (B) an array with 64 loops and 16 MTLs (Fig. 1). In both configurations, 16 stacks were arranged on a cylinder (25cm diameter). A 3D parametric coil design including all material properties, capacitors, and excitation ports was modeled using the CAD interface of HFSS 11 (Ansoft, Pittsburgh, PA). A stack in configuration A consists of one loop (5×20cm²) and one MTL (length 30cm; width 2cm) on a polypropylene plate (30×5×2cm³; $\varepsilon_r \approx 2.2$). A stack in configuration B consisted of 4 loops (5×5cm²) and one MTL (length 30cm; width 2cm). Each element was tuned and matched separately to 50Ω. Preamplifier decoupling was employed to minimize mutual couplings between stacked segments. A cylinder phantom with average values for the relative permittivity ($\varepsilon_r = 63.4$) and conductivity ($\sigma = 0.46$ S/m) of brain tissue was used as a load. The **E**- and **H**-fields in a cube around the phantom as obtained from HFSS as a solution of Maxwell's equations in the frequency domain were exported to MATLAB (The MathWorks, Natick, MA) for further processing. Coil sensitivities were calculated by $B_{xy} = (\mu_0/2)\,(H_x + \mathrm{i}\,H_y)$. As the mutual resistance matrix with elements $R_{ij} = \sigma/(I_i\,I_j) \iiint_V E_i\,E_j\,dV$ includes only sample losses, the complete resistance matrix was obtained by adding the copper losses of the array elements to the main diagonal. Often the mutual resistance matrix is represented as a noise correlation matrix, $\boldsymbol{\Psi}$, which is obtained after normalization according to $\Psi_{ij} = R_{ij}/(R_{ii}\,R_{jj})^{1/2}$ (2). For sum-of-squares reconstruction of a combined image, the SNR at location r is given by SNR = $\mathbf{s}'\,\mathbf{s}\,(\mathbf{s}'\,\boldsymbol{\Psi}\,\mathbf{s})^{-1/2}$, where $\mathbf{s}$ is a complex column vector of the coil sensitivities at location r (3).

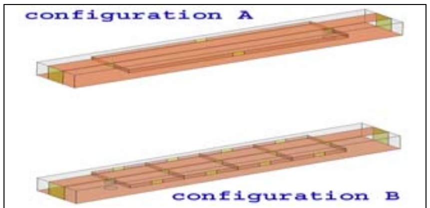

Fig. 1 Stack with one loop (conf. A) and with 4 loops (conf. B)

Results

The **E**-field distribution from the different antennas in the phantom is important for the noise level in the image. As shown in Fig. 2, the **E**-field is concentrated near the strip for the MTL, whereas the loop produces a strong **E**-field outside the central part of the loop. The **E**-field from the loop decreases with size and is orthogonal to that of the MTL. Therefore, the mutual resistance between an MTL and a loop antenna element is very low as seen in **Ψ** the matrix (Fig. 3A). For improving configuration A, the loop size can be reduced in *z*-direction, which also allows increasing the number of loops located at one stack. The advantage is twofold. Firstly, the range of the E-field into the head is reduced, which positively affects the electric coupling. Secondly, the additional coils with their non-uniform coil sensitivity profile will improve the possibilities of parallel imaging. We have chosen a number of 4 loops, which reasonably compromises between demanding and costly manufacturing on the one hand and the need of increasing the number of loops for improving the parallel imaging capabilities and SNR on the other hand. In configuration B, capacitive decoupling is employed by shared capacitors between neighboring loops. Additional preamp decoupling is used to suppress the coupling between next nearest neighbors. However, as seen in the **Ψ** the matrix, for configuration B with equal receiver phases for each loop on a stack, the mutual resistance between loop antennas is high (Fig. 3B) and only a subtle improvement in SNR in the outer parts of the phantom (Fig 4B, D) is obtained. Here, the performance of the coil can be improved, if phase differences of 90° are chosen for neighboring loops. As a consequence, the overlap of their respective **E**-fields is reduced, which manifests itself in the reduction of the related elements of the **Ψ** matrix (Figs. 3C). The immediate gain in SNR by about 25% can be seen (Figs. 4C & D) comparing the SNR obtained using the different two setups of configuration B, respectively. As an added advantage, the reduced size of the off-diagonal elements in **Ψ** the matrix will improve the parallel imaging performance.

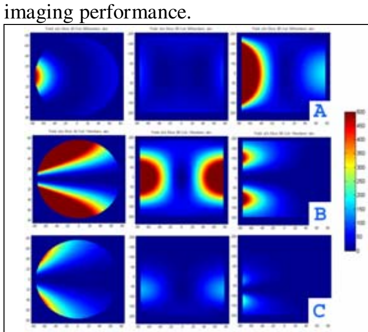

Fig. 2. Distribution of the amplitude of the **E**-field (left: axial; middle: coronal; right: sagittal slice): **(A)** MTL; **(B)** 20×5cm² loop; **(C)** 5×5cm² loop.

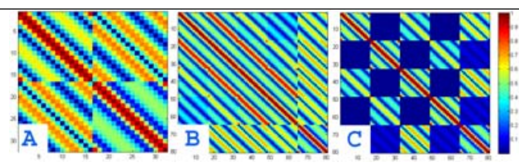

Fig. 3. Ψ-matrix: **(A)** 16 MTLs & 16 loops; (**B**) 16 MTLs & 64 loops (equal phases); **(C)** 16 MTLs & 64 loops (phase shifts: 0°, 90°, 180°, 270°).

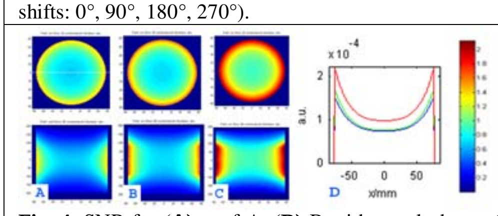

Fig. 4. SNR for (**A**) conf A**,** (**B**) B with equal phases **(C)** B with 90° phase shifts; (**D**) SNR along a central line for the maps in A (blue), B (green), C (red).

Conclusion

Simulations indicate that reasonable SNR performance can be achieved on outer parts of a phantom using small loops (configuration B). A remarkable improvement of SNR can be obtained when choosing optimized phases for neighboring loops, which requires only a simple modification (phase shifters).

Hardware or software channel-compression techniques or a selection of a subset of channels as a function of the FOV may be helpful for adapting configuration B with 80 elements to MRI systems equipped with only 32 or less receiver channels.

Acknowledgements

We thank H. Merkle and S. Wang for stimulating discussions on array design and calculation.

References: (1) W. Driesel & H.E. Möller, Proc. ISMRM 2008; 16:2977. (2) S. Wang et al., Phys. Med. Biol. 2008; 51:3211-29. S.B. King et al., Concepts Magn. Reson. Part B (Magn. Reson. Engineering) 2006; 29B:42–9.